

DOI: 10.1002/asia.201300738

Organorhodium-Functionalized Periodic Mesoporous Organosilica: High Hydrophobicity Promotes Asymmetric Transfer Hydrogenation in Aqueous Medium

Rui Liu, Ronghua Jin, Lingyu Kong, Jinyu Wang, Chen Chen, Tanyu Cheng,* and Guohua Liu*^[a]

Abstract: Three organosilica-bridged periodic mesoporous organosilicas were prepared by the immobilization of a chiral N-sulfonylated diamine-based organorhodium complex within their silicate network. Structural analysis and characterization confirmed their well-defined single-site active rhodium centers, whilst electron microscopy revealed their highly ordered hexagonal mesostructures. Among these three different organosilica-bridged periodic mesoporous organosilicas, the ethylene-bridged periodic mesoporous organosilica catalyst exhibited excellent

heterogeneous catalytic activity and high enantioselectivity in the aqueous asymmetric transfer hydrogenation of aromatic ketones. This superior catalytic performance was attributed to its salient hydrophobicity, whilst its comparable enantioselectivity relative to the homogeneous catalyst was derived from the confined nature of the chiral

organorhodium catalytic sites. Furthermore, this ethylene-bridged periodic mesoporous organosilica could be conveniently recovered and reused at least 12 times without the loss of its catalytic activity. This feature makes this catalyst attractive for practical organic synthesis in an environmentally friendly manner. This study offers a general way of optimizing the bridged organosilica moiety in periodic mesoporous organosilicas, thereby enhancing its catalytic activity in heterogeneous catalysis.

Keywords: asymmetric catalysis · heterogeneous catalysis · immobilization · mesoporous materials · silicas

Introduction

Periodic mesoporous organosilicas (PMOs) that contain chiral organic moieties embedded within their silicate networks have attracted a great deal of interest and have shown some salient features in asymmetric catalysis.^[1] Like inorganosilicate mesoporous materials,^[2] they also possess large specific surface areas/pore volumes, tunable pore dimensions/well-defined pore arrangements, and high thermal/mechanical stabilities. These properties open up a variety of possibilities for the immobilization of various homogeneous complexes onto periodic mesoporous organosilicas as supports.^[3] Unlike inorganosilicate mesoporous materials, periodic mesoporous organosilicas have a highly hydrophobic inner surface, owing to their intrinsic organosilicate walls, which may facilitate asymmetric reactions in a two-phase catalytic system and can promote organic transformations in

aqueous solution.^[4] More importantly, various organosilicate walls offer potential additional interactions with chiral active centers that are incorporated in the PMO silicate networks, such as π - π interactions and hydrogen bonds, which are beneficial for adjusting the chiral microenvironment around the active center and can enhance its enantioselective performance. Until now, although a large number of achiral-organosilica-bridged periodic mesoporous organosilicas have been reported^[5] and some periodic mesoporous organosilicas that incorporated chiral functionalities within their silica networks for asymmetric catalysis have also been explored,^[6] to the best of our knowledge, most of them still suffer from lower catalytic activities and enantioselectivities than their homogeneous counterparts. Thus, the utilization of the significant features of periodic mesoporous organosilica and the systemic adjustment of the organic bridge to achieve high catalytic activity and enantioselectivity remain unmet challenges in heterogeneous asymmetric catalysis.

We are interested in heterogeneous catalysts, in particular the development of various silica-based mesoporous heterogeneous catalysts. Recently, we have developed a series of inorganosilica-based chiral mesoporous heterogeneous catalysts, some of which have shown excellent catalytic activities and enantioselectivities in asymmetric reactions,^[7] in particular SBA-16-based chiral-organorhodium-functionalized mesoporous heterogeneous catalysts.^[7b] However, these inorga-

[a] Dr. R. Liu, Dr. R. Jin, Dr. L. Kong, Dr. J. Wang, Dr. C. Chen, Dr. T. Cheng, Prof. G. Liu
Key Laboratory of Resource Chemistry of
The Ministry of Education
Shanghai Key Laboratory of Rare Earth Functional Materials
Shanghai Normal University
Shanghai 200234 (P. R. China)

Supporting information for this article is available on the WWW under <http://dx.doi.org/10.1002/asia.201300738>.

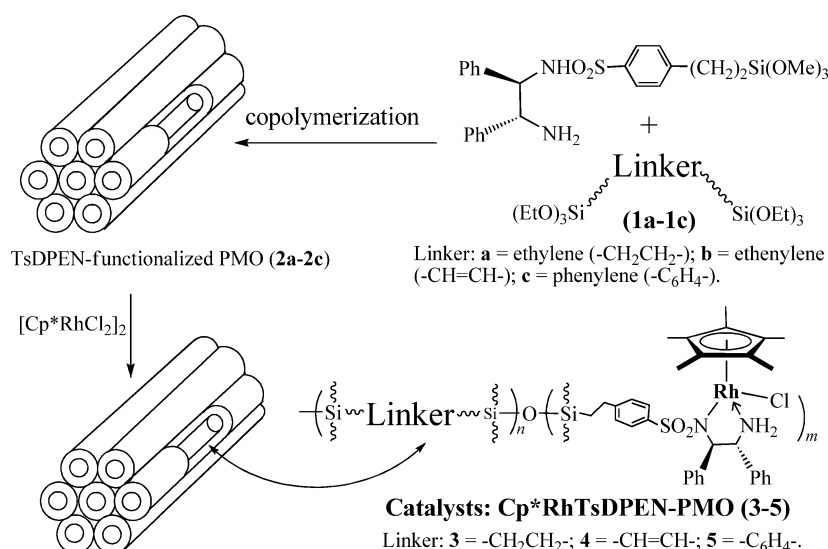
nosilica-based mesoporous chiral heterogeneous catalysts often showed low reaction rates, owing to the nature of the inorganosilicate materials. Interestingly, in organosilica-based chiral-organonickel-functionalized periodic mesoporous organosilica,^[8] the superior hydrophobicity of the periodic mesoporous organosilica affords much-higher catalytic performance in the asymmetric Michael addition of 1,3-dicarbonyl compounds to nitroalkenes. Herein, we utilize the salient hydrophobicity of periodic mesoporous organosilica to facilitate an asymmetric transfer-hydrogenation reaction in a typical two-phase catalytic system and

we develop three different organosilica-bridged chiral-Cp*RhTsDPEN-functionalized (Cp* = pentamethyl cyclopentadiene, TsDPEN = 4-methylphenylsulfonyl-1,2-diphenylethylenediamine) periodic mesoporous organosilicas.^[9] As expected, the superior hydrophobicity of these periodic mesoporous organosilicas affords greatly enhanced catalytic performance in the asymmetric transfer hydrogenation of aromatic ketones in aqueous medium. Moreover, by systematically optimizing the organosilica bridge, we found that ethylene-bridged chiral-Cp*RhTsDPEN-functionalized periodic mesoporous organosilica was the best chiral promoter, thereby affording excellent catalytic activity and comparable enantioselectivity to its homogeneous counterpart. Furthermore, this heterogeneous catalyst could be conveniently recovered and reused at least 12 times without loss of its catalytic activity, thus showing its potential industrial application. Moreover, a systemic comparison of three bridged periodic mesoporous organosilicas in terms of their enantioselective performance is also discussed in detail.

Results and Discussion

Synthesis and Structural Characterization of the Heterogeneous Catalysts

Three different organosilica-bridged N-sulfonylated diamine-based organorhodium-functionalized periodic mesoporous organosilicas, abbreviated as Cp*RhTsDPEN-PMO (**3–5**), were synthesized as shown in Scheme 1. Firstly, the key chiral TsDPEN-derived silane (*S,S*)-4-(trimethoxysilyl)ethylphenylsulfonyl-1,2-diphenylethylenediamine was obtained according to our previously reported procedure.^[7] Then, the co-condensation of TsDPEN-derived silane and various bridged silanes (**1a–1c**; **a**: 1,2-bis(triethoxysilyl)ethane, **b**: 1,2-bis(triethoxysilyl)ethylene, **c**: 1,4-bis(triethoxysilyl)benzene) afforded their corresponding TsDPEN-



Scheme 1. Synthesis of heterogeneous catalysts **3–5**.

functionalized PMOs (**2a–2c**) as white powders. Finally, heterogeneous catalysts **3–5** were successfully obtained by the direct complexation of [(Cp*RhCl₂)₂] with compounds **2a–2c**, followed by further Soxhlet extraction to clear their nanochannels (see the Supporting Information, Figures S1–S4).

The incorporation of well-defined single-site Cp*RhTsDPEN active centers within the organosilicate networks was confirmed by solid-state ¹³C cross-polarization (CP) magic angle spinning (MAS) NMR spectroscopy (see the Supporting Information, Figure S2). Taking TsDPEN-functionalized PMO **2a** and catalyst **3** as representative examples in Figure 1, we found that both compounds showed strong characteristic signals of the SiCH₂ groups at δ ≈ 7 ppm, which were ascribed to ethylene-bridged silica that was embedded within the silicate networks. A comparison of the spectrum of TsDPEN-functionalized PMO **2a** and catalyst **3** indicated that the peak at δ ≈ 95 ppm was derived from carbon atoms of the Cp rings, whilst the peak at δ ≈ 9 ppm corresponded to the carbon atoms of CH₃ groups

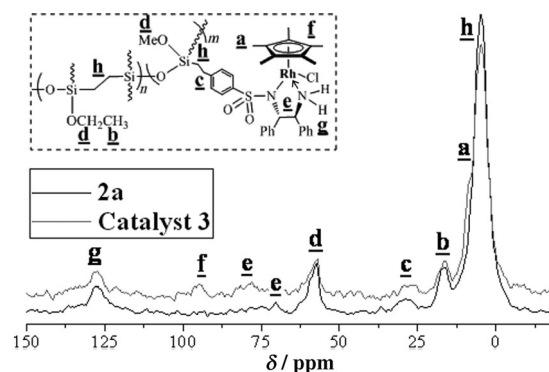


Figure 1. ¹³C CP MAS NMR spectra of TsDPEN-functionalized PMO **2a** and catalyst **3**.

that were connected to the Cp rings, thus suggesting that complexation of the CpMe₅ moiety and a chiral ligand had occurred. Moreover, catalyst **3** clearly displayed characteristic peaks at $\delta \approx 78$ –82 ppm, which corresponded to the carbon atoms of NCH groups that were connected to phenyl groups. In addition, the characteristic peaks at $\delta \approx 127$ ppm corresponded to the carbon atoms of the phenyl rings. Interestingly, in sharp contrast to the shifts of the signals for the CpMe₅ and NCH moieties,^[10] the spectrum of catalyst **3** was largely similar to that of its homogeneous counterpart, thus confirming that catalyst **3** had the same well-defined single-site active center. In addition, the peaks at $\delta \approx 16$ and 58 ppm should be attributed to nonhydrolyzed ethoxy groups (CH₃CH₂O) that often appear in the CP MAS spectra.^[11]

In addition, the organosilicate networks and compositions of heterogeneous catalysts **3**–**5** were confirmed by solid-state ²⁹Si MAS NMR spectroscopy (see the Supporting Information, Figure S3). As shown in Figure 2, TsDPEN-functional-

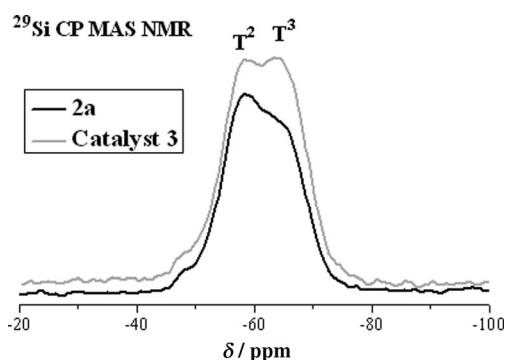


Figure 2. ²⁹Si CP MAS NMR spectra of TsDPEN-functionalized PMO **2a** and catalyst **3**.

ized PMO (**2a**) and catalyst **3** each showed one group of exclusive T signals that were derived from organosilica, thus suggesting that all of the Si species were covalently attached to carbon atoms.^[4] From a comparison with typical isomeric shifts reported in the literature^[12] ($\delta = -48.5$ – -58.5 / -67.5 ppm for T¹/T²/T³, [R(HO)₂SiOSi]/[R(HO)Si(OSi)₂]/[RSi(OSi)₃]), the T signals at $\delta = -58$ and -64 ppm corresponded to T² [RSi(OSi)₂(OH)] and T³ [RSi(OSi)₃] (R = Cp*RhTsDPEN or ethylene-bridged groups), respectively, similar to literature values.^[13] All of these observations demonstrated that TsDPEN-functionalized PMO **2a** and catalyst **3** possessed organosilicate networks with [RSi(OSi)₂(OH)] and [R-Si(OSi)₃] species as their main organosilicate walls. Furthermore, the absence of signals for the Q-series from $\delta = -90$ to -120 ppm indicated that no cleavage of the carbon–silicon bond occurred during the hydrolysis/condensation process.

To investigate the electronic state of the rhodium center, X-ray photoelectron spectroscopy (XPS) of catalysts **3**–**5** and its homogeneous counterpart (Cp*RhTsDPEN) were investigated. As shown in Figure 3, the XPS spectra of cata-

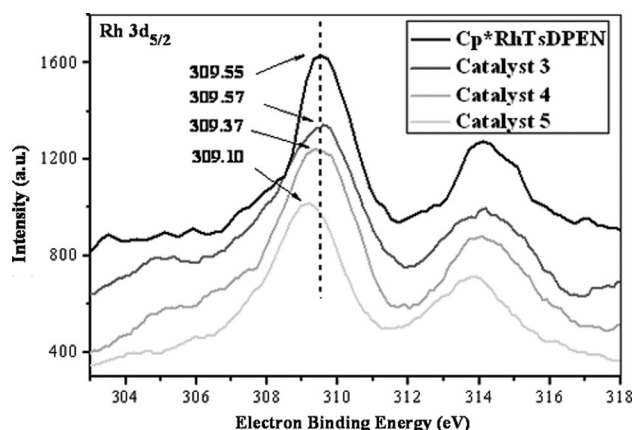


Figure 3. XPS spectra of Cp*RhTsDPEN and catalysts **3**–**5**.

lysts **3**–**5** presented similar Rh 3d_{5/2} binding energies to that of Cp*RhTsDPEN, which were clearly different from that of the parent [(Cp*RhCl₂)₂] (see the Supporting Information, Figure S5), thus demonstrating the formation of single-site Cp*RhTsDPEN active centers within their organosilicate networks. Notably, catalyst **3** had a comparable Rh 3d_{5/2} binding energy to its homogeneous counterpart (309.57 eV versus 309.55 eV), whilst catalysts **4** and **5** showed slight deviations from their homogeneous counterpart (309.10 and 309.37 eV versus 309.55 eV); these differences might be a key factor in determining their enantioselective performance (see below).

Furthermore, the ordered mesostructures and well-defined pore arrangements of these materials were further investigated by using X-ray diffraction (XRD), TEM, and nitrogen-adsorption/desorption techniques. As shown in Figure 4, the small-angle XRD patterns revealed that catalysts **3** and **4** presented one similar intense *d*₁₀₀ diffraction peak, along with two similar weak diffraction peaks (*d*₁₁₀, *d*₂₀₀), thus suggesting that the dimensional hexagonal pore structure (*p6mm*) that was observed in the pure PMO materials was preserved after co-condensation.^[8] The TEM morphologies of catalysts **3** and **4** further confirmed their well-ordered mesostructures with dimensional hexagonal ar-

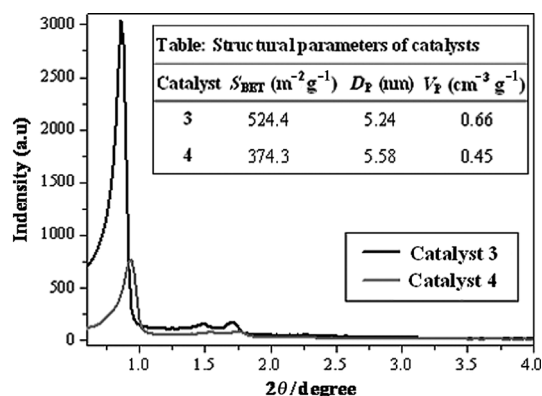


Figure 4. Small-angle powder-XRD patterns of catalysts **3** and **4**.

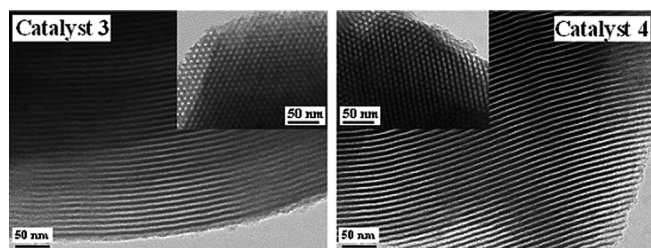


Figure 5. TEM images of catalysts **3** and **4**, viewed along the [100] and [001] directions.

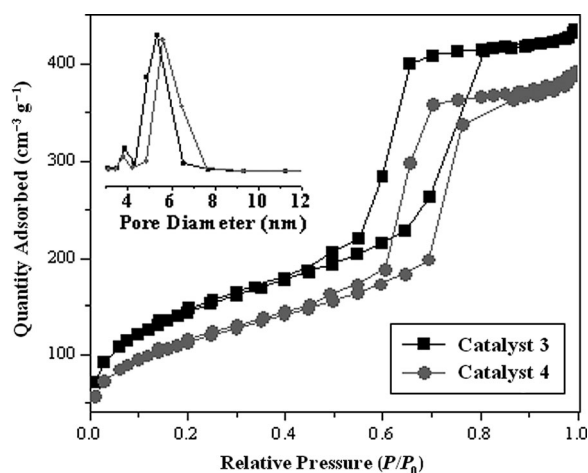


Figure 6. Nitrogen-adsorption/desorption isotherms of catalysts **3** and **4**.

rangements (Figure 5). In addition, the nitrogen-adsorption/desorption isotherms of catalysts **3** and **4** (Figure 6) exhibited typical type-IV isotherms with a H_1 hysteresis loop and a visible step at $P/P_0 = 0.50-0.90$, which corresponded to the capillary condensation of nitrogen in the mesopores; structural parameters are listed in Figure 4, inset. Similarly, an ordered mesostructure and well-defined pore arrangement were also observed for heterogeneous catalyst **5** (see the Supporting Information, Figure S6–S8). In particular, additional peaks were also observed at $2\theta = 10-50^\circ$ in the wide-angle powder XRD pattern for catalyst **5**, which could be assigned to a periodic phenylene-bridged structure and were very similar to literature values (see the Supporting Information, Figure S6).^[14]

Based on the above characterization and analysis, chiral organorhodium-functionalized periodic mesoporous organosilicas that contained well-defined single-site $\text{Cp}^*\text{RhTsDPEN}$ active centers in ordered dimensional hexagonal pore structures could be readily constructed with various types of bridged silane through a co-condensation strategy.

Catalytic Properties of the Heterogeneous Catalysts

Catalysts Screen and Catalytic Performance

As a type of highly active and enantioselective catalysts, chiral N-sulfonylated diamine-based organometallic compounds have been extensively studied in the asymmetric hydrogenation of ketones.^[9] Herein, we examined their catalytic activities and enantioselectivities in the aqueous asymmetric transfer hydrogenation of aromatic ketones according to a literature procedure,^[15] with which various chiral alcohols and their standard *ee* values have been established in our previous reports.^[7] Owing to their different types of bridging organosilicate walls, the as-prepared $\text{Cp}^*\text{RhTsDPEN-PMO}$ catalysts (**3–5**) were first screened in the asymmetric reaction of acetophenone; the reactions were performed by using 1.0 mol% of the catalyst in the absence of Bu_4NBr (Table 1, entry 1). Among these three heterogeneous catalysts, we found that the asymmetric reactions catalyzed by catalysts **4** and **5** afforded (*S*)-1-phenyl-1-ethanol with lower *ee* values than that of their homogenous counterpart. However, to our delight, catalyst **3** gave the corresponding products with 95% *ee*, comparable to that of its homogenous counterpart,^[15a] thus suggesting that ethylene-bridged heterogeneous catalyst **3** was the best promoter of this asymmetric reaction. Notably, the asymmetric reaction catalyzed by catalyst **3** could be performed at a much higher substrate/catalyst (S/C) ratio without affecting the *ee* value, as shown by the asymmetric transfer hydrogenation of acetophenone at S/C = 500:1 (Table 1, entry 1 in parentheses).

Table 1. Asymmetric transfer hydrogenation of aromatic ketones.^[a]

Entry	Substrate	Catalyst 3		Catalyst 4		Catalyst 5	
		Conversion [%] ^[b]	<i>ee</i> [%] ^[b]	Conversion [%] ^[b]	<i>ee</i> [%] ^[b]	Conversion [%] ^[b]	<i>ee</i> [%] ^[b]
1	Ph	>99 (92) ^[c]	95 (94) ^[c]	>99	91	>99	89
2 ^[d]	Ph	85	94	87	90	87	88
3 ^[e]	Ph	>99	94	>99	90	>99	88
4	4-FPh	>99	96	>99	90	>99	85
5	4-ClPh	>99	93	>99	91	>99	84
6	4-BrPh	>99	93	>99	85	>99	82
7	3-BrPh	>99	95	>99	92	>99	88
8	4-MePh	>99	96	>99	91	>99	89
9	4-	>99	95	>99	91	>99	85
10	OMePh						
	3-	>99	95	>99	90	>99	88
11	OMePh						
11	4-CNPh	>99	90	>99	80	98	78
12	4-NO ₂ Ph	>99	85	>99	79	95	72
13	4-CF ₃ Ph	>99	97	>99	84	>99	83

[a] Reaction conditions: Catalyst (2.00 μmol Rh based on ICP analysis), HCO_2Na (0.68 g, 10.0 mmol), ketone (0.20 mmol), water (2.0 mL), 40°C, 0.5–4.0 h. [b] Determined by chiral GC analysis (see the Supporting Information, Table S1 and Figure S9). [c] Homogeneous $\text{Cp}^*\text{RhTsDPEN}$ was used as the catalyst without the Bu_4NBr additive in aqueous medium. [d] S/C = 500:1. [e] TsDPEN-functionalized PMO **2a–2c** and $[(\text{Cp}^*\text{RhCl}_2)_2]$ were used as the catalysts. [f] TsDPEN-functionalized PMO **2a–2c** and homogeneous $\text{Cp}^*\text{RhTsDPEN}$ were used as the catalysts.

Based on these results, catalyst **3** was further investigated in the aqueous asymmetric transfer hydrogenation of various substituted acetophenones. In general, excellent conversions (with no side products) and high enantioselectivities were obtained under similar conditions. Moreover, the electronic properties of the substituents did not affect their enantioselectivities, that is, the asymmetric reactions with electron-rich and electron-poor substituents on acetophenone were equally efficient (Table 1, entries 4–13). For comparison, the asymmetric reactions catalyzed by catalysts **4** and **5** were also performed (Table 1, columns 4 and 5).

Investigation of the Nature of the Heterogeneous Catalysis

Generally, in a heterogeneous catalysis system, residual homogeneous catalyst often disturbs the catalytic nature of the heterogeneous catalysis through non-covalent physical adsorption during the preparation of the heterogeneous catalyst. In this case, to eliminate this possibility and to understand the nature of the heterogeneous catalysis, two types of parallel experiments, that is, reactions with TsDPEN-functionalized PMOs **2a–2c** plus $[(\text{Cp}^*\text{RhCl}_2)_2]$ and TsDPEN-functionalized PMOs **2a–2c** plus homogeneous $\text{Cp}^*\text{RhTsDPEN}$ as catalysts, were also investigated (Table 1, entries 2 and 3). Taking the reactions of compound **2a** plus $[(\text{Cp}^*\text{RhCl}_2)_2]$ and compound **2a** plus $\text{Cp}^*\text{RhTsDPEN}$ as examples, we found that the asymmetric reaction of acetophenone afforded the corresponding alcohol with 85% and >99% conversion, respectively, and 94% *ee* in both cases. The former reaction suggested that the catalyst that was synthesized through an in situ complexation method could lead to high enantioselectivity. The lower catalytic activity than that of catalyst **3** should be ascribed to the fact that part of $[(\text{Cp}^*\text{RhCl}_2)_2]$ was not coordinated during the catalysis process, in which the loss of Rh in solution was detected by ICP analysis. The latter case indicated that the homogeneous catalyst could result in good catalytic performance through non-covalent adsorption. However, when this catalyst underwent Soxhlet extraction, the reused catalyst only gave tiny products, clearly different from heterogeneous catalyst **3**. These results ruled out the role of noncovalent physical adsorption, thus demonstrating that the nature of the heterogeneous catalysis was indeed derived from the heterogeneous catalyst itself.

Investigation of the Factors that Affect Catalytic Performance

More attractively, the asymmetric reactions catalyzed by heterogeneous catalysts **3–5** presented clearly faster reaction rates than those of typical inorganosilica-based mesoporous heterogeneous catalysts.^[7a–d] In this case, owing to the salient hydrophobic features of heterogeneous catalysts **3–5**, the asymmetric reactions were performed in the absence of Bu_4NBr , unlike the homogeneous systems, which often needed Bu_4NBr as a phase-transfer catalyst to enhance their catalytic performance. Taking acetophenone as an example,

in the absence of Bu_4NBr , catalyst **3** gave (*S*)-1-phenyl-1-ethanol within 0.5 h with more than 99% conversion, higher than that with its homogeneous counterpart (88% conversion).^[7a] This improvement was more noticeable for the aqueous asymmetric reactions of 4-methoxyacetophenone. As reported previously,^[15a] this reaction needed 20 h to complete the asymmetric organic transformation, owing to its homogeneous catalytic nature. Herein, this asymmetric reaction of 4-methoxyacetophenone catalyzed by catalyst **3** was complete within 4.0 h. Notably, catalyst **3** showed a much-faster reaction rate than the homogeneous catalyst. To further confirm this result, the kinetic profiles for the asymmetric reaction of 4-methoxyacetophenone catalyzed by catalyst **3** and its homogeneous counterpart ($\text{Cp}^*\text{RhTsDPEN}$) were also investigated (Figure 7). These results showed that

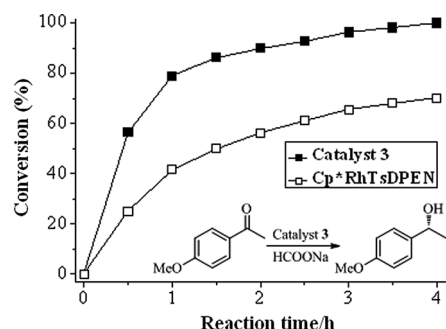


Figure 7. Comparison of the asymmetric transfer hydrogenation reactions of 4-methoxyacetophenone (squares) catalyzed by compound **3** and its homogeneous counterpart ($\text{Cp}^*\text{RhTsDPEN}$). The reactions were performed at 40°C with the catalyst (4.0 μmol , S/C = 500:1) and HCOONa (5 equiv) in water (2 mL).

catalyst **3** presented a higher initial activity than homogeneous $\text{Cp}^*\text{RhTsDPEN}$: The initial TOFs after 1.0 h were 394.5 and 208.0 $\text{mol}^{-1}\text{h}^{-1}$, respectively. Clearly, catalyst **3** showed a reaction rate that was almost twice that of its homogeneous counterpart, thus demonstrating that the enhanced reaction rate in this asymmetric organic transformations was attributed to its superior hydrophobicity; this result was confirmed by water/benzene gas-adsorption experiments and Pickering emulsion experiments (see the Supporting Information, Figures S10–S12).^[16]

Moreover, notably catalysts **3–5** showed clear differences in their enantioselective performance. As shown in Table 1, the asymmetric reaction catalyzed by catalyst **3** afforded higher enantioselectivities for all of the tested ketones than catalysts **4** and **5**. According to the elemental and ICP analyses, the total amount of chiral-organorhodium-functionalities that were used in these three asymmetric reactions was same; only the bridged organosilicate walls varied. Thus, a reasonable prediction is that the bridged organosilicate walls play an important role in determining their enantioselective performance. A possible explanation for this result is that the different organosilica-bridged functionalities offer different additional interactions with chiral active centers that are incorporated into their silicate networks, which

result in a change in the chiral microenvironment within the active center, thus affording differences in their enantioselective performance. Evidence to support this view came from X-ray photoelectron spectroscopy (XPS) investigations (Figure 3). Catalyst **3** had almost same Rh 3d_{5/2} binding energy as its homogeneous counterpart (309.57 eV versus 309.55 eV). As a result, catalyst **3** presented comparable enantioselectivity to its homogeneous counterpart. However, in the cases of heterogeneous catalysts **4** and **5**, the deviations in their Rh 3d_{5/2} electron-binding energies from those of their homogeneous counterparts (309.10 and 309.37 eV versus 309.55 eV) were responsible for their low enantioselectivities, owing to changes in the chiral microenvironment within the active center. Among these three heterogeneous catalysts, the main compositional differences were that catalysts **4** and **5** had unsaturated ethylene- or phenylene-bridged organosilicas as their silica walls, whilst catalyst **3** had saturated ethylene-bridged organosilica as its silica walls. Clearly, in catalysts **4** and **5**, there were potential π - π interactions^[5c] between ethylene- or phenylene-bridged moieties and the Ph group of 1,2-diphenylethylenediamine, which enforced a certain configurational transformation of the active center, thereby resulting in a decrease in facial selectivity. To confirm the presence of such π - π interactions, a comparable inorganosilica-based SBA-15-type mesoporous heterogeneous catalyst was prepared by using a similar strategy, in which inorganosilicate O-Si-O groups acted as its silicate walls rather than ethylene- or phenylene-bridged organosilicate moieties. These results showed that the *ee* value returned to normal value (95% *ee*)^[7d] when the comparable inorganosilica-based SBA-15-type mesoporous heterogeneous catalyst was employed in the asymmetric transfer hydrogenation of acetophenone, thus demonstrating that the π - π interactions in catalysts **4** and **5** were responsible for their lower enantioselectivities.

Catalyst Recycling and Reuse

An important feature of any heterogeneous catalyst is its easy separation by simple filtration and the recovered catalyst should retain its catalytic activity and enantioselectivity after multiple cycles. As shown in Table 2, heterogeneous catalyst **3** was easily recovered and repeatedly reused when acetophenone was chosen as the substrate. Remarkably, after 12 consecutive reactions, the recycled catalyst still afforded (*S*)-1-phenyl-1-ethanol with 99% conversion and 92% *ee*. Notably, this high recyclability should be due to the

Table 2. Reusability of catalyst **3** in the asymmetric transfer hydrogenation of acetophenone.^[a,b]

Run	1	2	3	4	5	6	7	8	9	10	11	12
Conversion [%]	99.9	99.9	99.9	99.9	99.9	99.9	99.9	99.9	99.9	99.9	99.9	99.9
<i>ee</i> [%]	95.0	94.6	94.4	94.0	93.7	93.3	93.4	93.3	93.0	92.7	92.3	92.2

[a] Reaction conditions: catalyst **3** (73.5 mg, 20.0 μ mol Rh based on ICP analysis), HCO₂Na (0.68 g, 100.0 mmol), acetophenone (2.0 mmol), water (20.0 mL), 40°C, 0.5–4.0 h. [b] Determined by chiral GC analysis (see the Supporting Information, Figure S13).

fact that this co-condensation strategy, which proceeded through a covalent-bonding immobilization approach, could efficiently decrease the leaching of Rh. Evidence to support this view came from ICP analysis, which showed that the amount of Rh after the 13th cycle was 26.97 mg per gram of catalyst and only 3.7% of the Rh content was lost, thus demonstrating that its high recyclability was attributed to the low leaching of Rh. Similarly, heterogeneous catalysts **4** and **5** were easily recovered and repeatedly reused when acetophenone was chosen as a substrate. Recycled catalysts **4** and **5** retained their catalytic activities and enantioselectivities after eight cycles (see the Supporting Information, Table S2).

Conclusions

In conclusions, three organosilica-bridged chiral-Cp**Rh*TsDPEN-functionalized periodic mesoporous organosilicas have been prepared and their use in the aqueous asymmetric transfer hydrogenation of aromatic ketones has been investigated. As expected, these three heterogeneous catalysts showed excellent catalytic performance, owing to the hydrophobic nature of the periodic mesoporous organosilica, whilst the additional π - π interactions between the unsaturated ethylene-bridged or phenylene-bridged organosilica and the phenyl moiety on the chiral ligand played an important role in their enantioselective performance. Furthermore, ethylene-bridged heterogeneous catalyst **3** could be conveniently recovered and reused at least 12 times without loss of its catalytic activity. This study offers a general way of optimizing the bridging organosilane moiety in periodic mesoporous organosilicas to tune their catalytic activity in heterogeneous reactions.

Experimental Section

Preparation of (*S,S*)-TsDPEN-Functionalized PMO **2a**

In a typical synthesis, the structure-directing agent pluronic P123 (2.0 g) was completely dissolved in a mixture of 0.2 M HCl (80 mL) and KCl (6.0 g) and the mixture was stirred at RT for 1.0 h. Then, 1,2-bis(triethoxysilyl)ethane (3.36 mL, 9.10 mmol) was added as the silica precursor at 40°C. After a pre-hydrolysis period of 40 min, (*S,S*)-DPEN-SO₂Ph-(CH₂)₂Si(OMe)₃ (0.48 g, 0.96 mmol) was added. The reaction mixture was stirred at 40°C for 24 h and aged at 100°C for 24 h. The resulting solid was filtered and rinsed with excess EtOH before being dried overnight on a filter. The surfactant template was removed by heating at reflux in acidic EtOH (400 mL g⁻¹) for 24 h. The solid was filtered, rinsed again with EtOH, and dried at 60°C overnight under reduced pressure to afford TsDPEN-functionalized PMO material **2a** (1.42 g) as a white powder. ²⁹Si MAS NMR (79.4 MHz): T² (δ = -58.6 ppm), T³ (δ = -63.9 ppm); ¹³C CP MAS NMR (161.9 MHz): δ = 127.4 (CH of Ph), 74.8, 70.1 (NCHPh), 57.4 (OCH₂CH₃), 28.8 (CH₂Ph), 16.6 (OCH₂CH₃), 14.6–0.5 ppm (CH₂Si); IR (KBr): $\tilde{\nu}$ = 3434.4 (s), 2986.0 (w), 2896.0 (w), 1657.6 (m), 1415.6 (w), 1263.3 (m), 1155.2 (s), 1068.7 (s), 913.1 (m), 766.1 (m), 697.7 (s), 448.1 cm⁻¹ (m); *S*_{BET} = 618.7 m² g⁻¹; *d*_{pore} = 5.59 nm; *V*_{pore} = 0.72 cm³ g⁻¹.

Preparation of (S,S)-TsDPEN-Functionalized PMO **2b**

Compound **2b** was prepared according to the general procedure for compound **2a** by using 1,2-bis(triethoxysilyl)ethane instead of 1,2-bis(triethoxysilyl)ethane. The solid was dried overnight under reduced pressure to afford compound **2b** as a white powder; ^{29}Si MAS NMR (79.4 MHz): T^1 ($\delta = -63.5$ ppm), T^2 ($\delta = -72.5$ ppm), T^3 ($\delta = -81.5$ ppm); ^{13}C CP MAS NMR (161.9 MHz): $\delta = 145.8$ (CH of Ph), 132.9 (CH=CH), 72.2, 69.9 (NCHPh), 58.7 (OCH₂CH₃), 30.7 (CH₂Ph), 20.8–10.5 ppm (OCH₂CH₃ and CH₂Si); IR (KBr): $\tilde{\nu} = 3416.8$ (s), 3084.2 (w), 2976.8 (w), 2931.9 (w), 1657.6 (m), 1496.3 (w), 1433.8 (w), 1388.9 (w), 1155.2 (s), 1074.5 (s), 922.2 (m), 814.2 (m), 679.4 (m), 518.0 cm⁻¹ (m); $S_{\text{BET}} = 412.5$ m² g⁻¹; $d_{\text{pore}} = 5.65$ nm; $V_{\text{pore}} = 0.58$ cm³ g⁻¹.

Preparation of Heterogeneous Catalyst **3**

In a typical synthesis, to a stirring suspension of TsDPEN-functionalized PMO material **2a** (1.0 g) in dry CH₂Cl₂ (20 mL) was added [(Cp*RhCl₂)₂] (0.10 g, 0.16 mmol) at RT. The resulting mixture was stirred at RT for 12 h. Then, the mixture was filtered through filter paper and rinsed with excess CH₂Cl₂ and dry toluene. After Soxhlet extraction in toluene to remove homogeneous and unreacted starting materials for 24 h, the solid was dried at 60 °C overnight under vacuum to afford catalyst **3** (1.04 g) as a light-yellow powder. ICP analysis showed that the Rh loading was 28.01 mg (0.272 mmol) per gram of catalyst. ^{29}Si MAS NMR (79.4 MHz): T^2 ($\delta = -58.4$ ppm), T^3 ($\delta = -63.7$ ppm); ^{13}C CP MAS NMR (161.9 MHz): $\delta = 127.3$ (CH of Ph), 94.4 (C of Cp ring), 81.3, 77.7 (NCHPh), 57.4 (OCH₂CH₃), 27.7 (CH₂Ph), 16.1 (OCH₂CH₃), 8.8 (CpCH₃), 14.6–0.5 ppm (CH₂Si); IR (KBr): $\tilde{\nu} = 3429.2$ (s), 2978.8 (w), 2896.3 (w), 1657.1 (m), 1409.2 (w), 1271.6 (m), 1160.9 (s), 1087.7 (s), 913.3 (m), 766.8 (m), 702.2 (s), 445.3 cm⁻¹ (m); $S_{\text{BET}} = 524.4$ m² g⁻¹; $d_{\text{pore}} = 5.24$ nm; $V_{\text{pore}} = 0.66$ cm³ g⁻¹.

Preparation of Heterogeneous Catalyst **4**

Catalyst **4** was prepared according to the general procedure for catalyst **3**. The solid was dried overnight under reduced pressure to afford catalyst **4** as a brown powder. ICP analysis showed that the Rh loading was 39.04 mg (0.379 mmol) per gram of catalyst. ^{29}Si MAS NMR (79.4 MHz): T^1 ($\delta = -65.2$ ppm), T^2 ($\delta = -74.6$ ppm), T^3 ($\delta = -82.6$ ppm); ^{13}C CP MAS NMR (161.9 MHz): $\delta = 146.4$ (CH=CH), 128.1 (CH of Ph), 94.7 (C of Cp ring), 78.6, 75.5 (NCHPh), 58.2 (OCH₂CH₃), 28.6 (CH₂Ph), 20.8–10.5 (OCH₂CH₃ and CH₂Si), 9.2 ppm (CpCH₃); IR (KBr): $\tilde{\nu} = 3392.5$ (s), 3089.5 (w), 2978.8 (w), 2942.3 (w), 1647.7 (m), 1455.4 (w), 1427.3 (w), 1381.4 (w), 1160.9 (s), 1069.8 (s), 922.6 (m), 794.1 (m), 435.8 cm⁻¹ (m); $S_{\text{BET}} = 374.3$ m² g⁻¹; $d_{\text{pore}} = 5.58$ nm; $V_{\text{pore}} = 0.45$ cm³ g⁻¹.

General Procedure for the Asymmetric Transfer Hydrogenation of Aromatic Ketones

A typical procedure is as follows: Heterogeneous catalyst **3** (2.00 μmol Rh based on ICP analysis), HCO₂Na (0.68 g, 10.0 mmol), ketone (0.2 mmol), and water (2.0 mL) were successively added into a 10 mL round-bottomed flask. The mixture was heated at 40 °C for 0.5–4.0 h, during which time the reaction was monitored by TLC. After completion of the reaction, the heterogeneous catalyst was separated by centrifugation (10000 r min⁻¹) for the recycling experiment. The aqueous solution was extracted with Et₂O (3 × 3.0 mL). The combined Et₂O was washed twice with brine and dehydrated with Na₂SO₄. After the evaporation of Et₂O, the residue was purified by column chromatography on silica gel to afford the desired product. The conversion and *ee* value were determined by chiral GC on a chiral Supelco β-Dex 120 column (30 m × 0.25 mm i.d., 0.25 μm film) or by HPLC analysis with a UV/Vis detector on a Daicel OD-H chiralcel column ($\phi = 0.46 \times 25$ cm).

Acknowledgements

We are grateful to the National Natural Science Foundation of China (20673072), the Shanghai Sciences and Technologies Development Fund

(10J1400103, 10JC1412300, and 12nm0500500), the CSIRT (IRT1269), and the Shanghai Municipal Education Commission (12ZZ135 and SK201329) for financial support.

- [1] a) A. Thomas, *Angew. Chem.* **2010**, *122*, 8506; *Angew. Chem. Int. Ed.* **2010**, *49*, 8328; b) N. Mizoshita, T. Taniab, S. Inagaki, *Chem. Soc. Rev.* **2011**, *40*, 789; c) F. Hoffmann, M. Fröba, *Chem. Soc. Rev.* **2011**, *40*, 608; d) F. Hoffmann, M. Cornelius, J. Morell, M. Fröba, *Angew. Chem.* **2006**, *118*, 3290; *Angew. Chem. Int. Ed.* **2006**, *45*, 3216; e) M. Kruk, *Acc. Chem. Res.* **2012**, *45*, 1678; f) J. A. Melero, R. van Grieken, G. Morales, *Chem. Rev.* **2006**, *106*, 3790–3812; g) Q. Yang, J. Liu, L. Zhang, C. Li, *J. Mater. Chem.* **2009**, *19*, 1945; h) P. Van Der Voort, D. Esquivel, E. De Canck, F. Goethals, I. Van Driessche, F. J. Romero-Salguero, *Chem. Soc. Rev.* **2013**, *42*, 3913.
- [2] a) F. Kleitz in *Handbook of Asymmetric Heterogeneous Catalysis*, Wiley-VCH, Weinheim, **2008**, pp. 178; b) D. E. De Vos, M. Dams, B. F. Sels, P. A. Jacobs, *Chem. Rev.* **2002**, *102*, 3615; c) H. Zou, S. S. Wu, J. Shen, *Chem. Rev.* **2008**, *108*, 3893; d) S. Minakata, M. Komatsu, *Chem. Rev.* **2009**, *109*, 711; e) A. Corma, *Chem. Rev.* **1997**, *97*, 2373; f) J. M. Thomas, R. Raja, *Acc. Chem. Res.* **2008**, *41*, 708; g) C. Li, H. D. Zhang, D. M. Jiang, Q. H. Yang, *Chem. Commun.* **2007**, 547.
- [3] a) M. E. Davis, *Nature* **2002**, *417*, 813; b) S. Inagaki, S. Guan, T. Ohsuna, O. Terasaki, *Nature* **2002**, *416*, 304.
- [4] a) J. L. Huang, F. X. Zhu, W. H. He, F. Zhang, W. Wang, H. X. Li, *J. Am. Chem. Soc.* **2010**, *132*, 1492; b) X. S. Yang, F. X. Zhu, J. L. Huang, F. Zhang, H. X. Li, *Chem. Mater.* **2009**, *21*, 4925.
- [5] a) Y. F. Lu, H. Y. Fan, N. Doke, D. A. Loy, R. A. Assink, D. A. Lavan, C. J. Brinker, *J. Am. Chem. Soc.* **2000**, *122*, 5258; b) B. D. Hatton, K. Landskron, W. Whitnall, D. D. Perovic, G. A. Ozin, *Adv. Funct. Mater.* **2005**, *15*, 823; c) M. P. Kapoor, Q. H. Yang, S. Inagaki, *J. Am. Chem. Soc.* **2002**, *124*, 15176; d) P. Borah, X. Ma, K. T. Nguyen, Y. Zhao, *Angew. Chem.* **2012**, *124*, 7876; *Angew. Chem. Int. Ed.* **2012**, *51*, 7756; e) M. Waki, N. Mizoshita, T. Tani, S. Inagaki, *Angew. Chem.* **2011**, *123*, 11871; *Angew. Chem. Int. Ed.* **2011**, *50*, 11667; f) M. Guan, W. Wang, E. J. Henderson, Ö. Dag, C. Kübel, V. S. K. Chakravadhanula, J. Rinck, I. L. Moudrakovski, J. Thomson, J. McDowell, A. K. Powell, H. Zhang, G. A. Ozin, *J. Am. Chem. Soc.* **2012**, *134*, 8439; g) M. Mandal, M. Kruk, *Chem. Mater.* **2012**, *24*, 123.
- [6] a) A. Kuschel, S. Polarz, *J. Am. Chem. Soc.* **2010**, *132*, 6558; b) X. Wu, T. Blackburn, J. D. Webb, A. E. Garcia-Bennett, C. M. Crudden, *Angew. Chem.* **2011**, *123*, 8245; *Angew. Chem. Int. Ed.* **2011**, *50*, 8095; c) X. Liu, P. Y. Wang, L. Zhang, J. Yang, C. Li, Q. H. Yang, *Chem. Eur. J.* **2010**, *16*, 12727; d) R. A. Garcia, R. van Grieken, J. Iglesias, V. Morales, N. Villajos, *J. Catal.* **2010**, *274*, 221; e) P. Y. Wang, X. Liu, J. Yang, Y. Yang, L. Zhang, Q. H. Yang, C. Li, *J. Mater. Chem.* **2009**, *19*, 8009; f) T. Seki, K. McEleney, C. M. Crudden, *Chem. Commun.* **2012**, *48*, 6369.
- [7] a) H. S. Zhang, R. H. Jin, H. Yao, S. Tang, J. L. Zhuang, G. H. Liu, H. X. Li, *Chem. Commun.* **2012**, *48*, 7874; b) W. Xiao, R. H. Jin, T. Y. Cheng, D. Q. Xia, H. Yao, F. Gao, B. X. Deng, G. H. Liu, *Chem. Commun.* **2012**, *48*, 11898; c) Y. Q. Sun, G. H. Liu, H. Y. Gu, T. Z. Huang, Y. L. Zhang, H. X. Li, *Chem. Commun.* **2011**, *47*, 2583; d) J. Long, G. H. Liu, T. Y. Cheng, H. Yao, Q. Q. Qian, J. L. Zhuang, F. Gao, H. X. Li, *J. Catal.* **2013**, *298*, 41; e) S. Tang, R. H. Jin, H. S. Zhang, H. Yao, J. L. Zhuang, G. H. Liu, H. X. Li, *Chem. Commun.* **2012**, *48*, 6286; f) G. H. Liu, J. Y. Wang, T. Z. Huang, X. H. Liang, Y. L. Zhang, H. X. Li, *J. Mater. Chem.* **2010**, *20*, 1970; g) D. Q. Xia, T. Y. Cheng, W. Xiao, K. K. Liu, Z. L. Wang, G. H. Liu, H. L. Li, W. Wang, *ChemCatChem* **2013**, *5*, 1784–1789; h) Y. L. Xu, T. Y. Cheng, J. Long, K. T. Liu, Q. Q. Qian, F. Gao, G. H. Liu, H. X. Li, *Adv. Synth. Catal.* **2012**, *354*, 3250.
- [8] a) R. H. Jin, K. T. Liu, D. Q. Xia, Q. Q. Qian, G. H. Liu, H. X. Li, *Adv. Synth. Catal.* **2012**, *354*, 3265; b) K. T. Liu, R. H. Jin, T. Y. Cheng, X. M. Xu, F. Gao, G. H. Liu, H. X. Li, *Chem. Eur. J.* **2012**, *18*, 15546.

- [9] a) T. Ikariya, A. J. Blacker, *Acc. Chem. Res.* **2007**, *40*, 1300; b) J. E. D. Martins, G. J. Clarkson, M. Wills, *Org. Lett.* **2009**, *11*, 847; c) R. Malacea, R. Poli, E. Manoury, *Coord. Chem. Rev.* **2010**, *254*, 729.
- [10] J. Mao, D. C. Baker, *Org. Lett.* **1999**, *1*, 841.
- [11] P. F. W. Simon, R. Ulrich, H. W. Spiess, U. Wiesner, *Chem. Mater.* **2001**, *13*, 3464.
- [12] O. Kröcher, O. A. Köppel, M. Fröba, A. Baiker, *J. Catal.* **1998**, *178*, 284.
- [13] a) B. J. Melde, B. T. Holland, C. F. Blanford, A. Stein, *Chem. Mater.* **1999**, *11*, 3302; b) N. Linares, A. E. Sepúlveda, J. R. Berenguer, E. Lalinde, J. Garcia-Martinez, *Microporous Mesoporous Mater.* **2012**, *158*, 300.
- [14] a) Q. Yang, M. P. Kapoor, S. Inagaki, *J. Am. Chem. Soc.* **2002**, *124*, 9694.
- [15] a) X. F. Wu, X. H. Li, A. Zanotti-Gerosa, A. Pettman, J. Liu, A. J. Mills, J. L. Xiao, *Chem. Eur. J.* **2008**, *14*, 2209; b) X. F. Wu, J. Liu, D. D. Tommaso, J. A. Iggo, C. R. Catlow, J. Bacsá, J. L. Xiao, *Chem. Eur. J.* **2008**, *14*, 7699; c) P. N. Liu, J. G. Deng, Y. Q. Tu, S. H. Wang, *Chem. Commun.* **2004**, 2070; d) N. A. Cortez, G. Aguirre, M. Parra-Hake, R. Somanathan, *Tetrahedron Lett.* **2009**, *50*, 2228.
- [16] a) Y. Kuwahara, J. Aoyama, K. Miyakubo, T. Eguchi, T. Kamegawa, K. Mori, H. Yamashita, *J. Catal.* **2012**, *285*, 223; b) L. A. Fielding, S. P. Armes, *J. Mater. Chem.* **2012**, *22*, 11235.

Received: June 1, 2013

Revised: July 4, 2013

Published online: September 2, 2013